encit 2020

ABCM Associação Brasileira de Engenharia e Ciências Mecânicas

18th Brazilian Congress of Thermal Sciences and Engineering
November 16-20, 2020 (Online)

ENC-2020-0534
COMPARISON OF GG AND WSGG MODELS FOR GAS AND SOOT RADIATION IN COUPLED POOL FIRE SIMULATIONS

Felipe Robinson Silva
Guilherme Crivelli Fraga
Felipe Roman Centeno
Federal University of Rio Grande do Sul, Mechanical Engineering Department - 425 Sarmento Leite St., Porto Alegre, RS, Brazil
felipe.robinson@ufrgs.br
guilhermecfraga@gmail.com
frcenteno@mecanica.ufrgs.br

Abstract. *Fully-coupled large eddy simulations of a* $30\,\text{cm} \times 30\,\text{cm}$ *square-shaped ethanol pool fire are carried out with the purpose of comparing different spectral models for the treatment of the radiative transfer. Both the gray gas (GG) model and the non-gray weighted-sum-of-gray-gases (WSGG) model are considered. Four calculations with the gray gas model (considering and neglecting soot formation and a correction to the radiative emission term to account for underpredicted flame temperatures due to coarse grid) and another with the WSGG have been carried out. Results show that the GG solutions are much closer to each other than to the WSGG model, signaling that the gas radiation has considerably more importance than the soot radiation (that displays a near-gray spectral behavior) for the flame under study. On the other hand, soot formation has more impact over the results than including the radiative emission correction. The smaller radiation losses predicted by the WSGG model led to larger differences to the experimental data when compared to the GG models, likely because of errors introduced by models for other physical simulations processes.*

Keywords: *Thermal radiation, pool fires, weighted-sum-of-gray-gases model, gray gas model*

1. INTRODUCTION

Thermal radiation is one of the major heat transfer modes in the combustion processes, due to the high-temperatures involved and to the presence of species, such as water vapor and carbon dioxide, that participate in the radiative exchange (Modest and Haworth, 2016). The determination of the radiation field usually entails the solution of the radiative transfer equation (RTE), an integro-differential equation in six dimensions (three spatial directions, two directional coordinates and an additional spectral dependence). Further complicating this is the fact that the radiative properties of gases such as H_2O and CO_2 present a very complex dependence on the radiation spectrum, characterized by hundreds of thousands to millions of absorption lines (Modest, 2013; Howell *et al.*, 2016).

The spectral part of the problem (i.e., capturing the variations of the radiative properties across the spectrum) can be solved with a high degree of accuracy through the line-by-line method (LBL). This method consists of solving the RTE in its spectral form for each absorption line, which has the drawback of dramatically increasing the computational cost of the radiation solver. This makes the LBL method prohibitive for practical applications, particularly for three-dimensional simulations that also need to resolve other complex processes such as turbulence or combustion.

Therefore, models to simplify the spectral treatment of the radiative transfer have been introduced, the most simple of which being the gray gas (GG) model. In this model, spectral variations of the radiative properties are outright neglected, which greatly simplifies the solution of the radiation field. Although the GG approach is known to lead to large errors for modeling gas radiation, it still is one of the most commonly used methodologies for computing the radiative transfer in combustion and fire applications (Modest and Haworth, 2016). An alternative to the GG model that allows the consideration of the spectral dependence of radiative transfer problem is the weighted-sum-of-gray-gases (WSGG) model (Modest, 1991). In this model, the participating medium is represented by a small number of gray gases for which the RTE can be solved separately. Since fairly accurate results can often be obtained even when using a small number of gray gases, the WSGG model does not incur in an excessive computational cost, and thus has been widely used in the radiation community.

In the present paper, the GG and WSGG models are tested for the simulation of a laboratory-scale ethanol pool fire. This pool fire has been the subject of previous experimental investigation (Tu *et al.*, 2013), and, recently, Fernandes *et al.*, 2020, compared the performance of different formulations of the GG model for its simulation. Here, besides variants of the GG model, the WSGG model is also tested. All simulations are transient, with the flow, thermal and combustion

problems solved in a coupled manner, and turbulence is modeled via the large eddy simulation methodology.

2. PROBLEM STATEMENT

The problem under study in this paper is based on the configuration experimentally studied by Tu *et al.*, 2013. A 0.3 m-side, 14 mm-deep square-shaped pool containing 1 kg of liquid ethanol burns in air inside a closed compartment with dimensions 10 m long, 7 m wide and 4 m high. In Tu *et al.*, 2013, the fuel mass loss rate of this flame was measured as approximately 18 g/(m^2 s), and the radiant fraction of the flame was estimated to be 0.2.

3. PHYSICAL MODELING

3.1 Turbulent flow and combustion

Favre-filtered transport equations for species mass fraction, momentum and energy are solved for a three-dimensional, low-Mach number, compressible flow in a Cartesian coordinate system (McGrattan *et al.*, 2019a). The spatial filtering required for the large eddy simulation (LES) methodology is defined by a low-pass box filter of width comparable to the grid cell size. The closure of the Navier-Stokes equation is achieved via the dynamic Smagorinsky model (Germano *et al.*, 1991), and a gradient diffusion assumption is invoked to model the subfilter-scale species and enthalpy fluxes, with constant turbulent Prandtl and Schmidt numbers. A single-step, complete reaction of fuel and air describes the combustion mechanism. To reduce the computational cost of the simulations a lumped species approach is adopted, with the filtered reaction rate of each species determined assuming infinitely-fast, mixing-controlled chemistry through the eddy dissipation concept model (Magnussen and Hjertager, 1977). Further detail on the physical models employed in the present simulations can be found in McGrattan *et al.*, 2019a, and Fernandes *et al.*, 2020.

3.2 Thermal radiation

Coupling of the thermal radiation to the transport equations is given by the volumetric radiative heat source, S_r, which is defined as the symmetric of the divergent of the radiative heat flux vector, or (Modest, 2013)

$$S_r = \kappa_G G - 4\pi\kappa_P I_b \,, \tag{1}$$

where I_b is the blackbody radiation intensity, G is the incident radiation, and κ_G and κ_P are the incident-mean and Planck-mean absorption coefficients, respectively. The blackbody radiation intensity is a simple function of the local temperature T, $I_b = \sigma T^4/\pi$ (where σ is the Stefan-Boltzmann constant), while the incident radiation is defined as the local intensity I integrated over all solid angles Ω, $G = \int_{4\pi} I \,\mathrm{d}\Omega$. To determine the radiation intensity itself, the radiative transfer equation (RTE) is solved, which, assuming a non-scattering and isotropic medium, is expressed as

$$\frac{\mathrm{d}I}{\mathrm{d}s} = -\kappa_G I + \kappa_P I_b \,, \tag{2}$$

where s is the path of radiation propagation. Note that the condition of isotropic radiation is only included here to simplify how Eq. (2) is written, and it is not necessary for the actual simulations of the present study.

The direction and spatial integrations of Eq. (2) are carried out with the finite volume method (FVM) (Raithby and Chui, 1990). To represent the dependence of the radiative properties of the medium—given by the κ_G and κ_P coefficients for the RTE as it is expressed in Eq. (2)—two spectral models are used: the gray gas (GG) and the weighted-sum-of-gray-gases (WSGG) models. In the former, variations of the absorption coefficient of the medium in the radiation spectrum are outright neglected, hence $\kappa_G = \kappa_P = \kappa$ and the RTE reduces to

$$\frac{\mathrm{d}I}{\mathrm{d}s} = \kappa(I_b - I) \,. \tag{3}$$

A well-established correlation, proposed by Cassol *et al.*, 2015, is adopted to describe the functional dependence of κ on the local thermodynamic state (e.g., the temperature, pressure and medium composition).

The WSGG model, on the other hand, is capable of taking the spectral dependence of the radiative transfer problem into account. It does so by representing the absorption spectrum of the participating medium by a set of J gray gases plus some transparent windows. Then, the RTE solved for each gray gas has the form (Modest, 1991)

$$\frac{\mathrm{d}I_j}{\mathrm{d}s} = -\kappa_j I_j + \kappa_j a_j I_b \,, \tag{4}$$

in which I_j is the partial radiation intensity associated to the jth gas, and κ_j and a_j are the absorption coefficient and blackbody weighting coefficient of the gas, respectively. The latter coefficient corresponds the fraction of blackbody energy that is emitted in the spectral regions belonging to the jth gray gas, and is often expressed as a polynomial function

of the local temperature. Once Eq. (4) has been solved for each individual gray gas, the total radiation intensity is obtained as $I = \sum_{j=0}^{J} I_j$, with $j = 0$ denoting the transparent windows, for which $\kappa_0 = 0$ and $a_0 = 1 - \sum_{j=1}^{J} a_j$.

The WSGG formulation of Centeno *et al.*, 2018, is adopted in the present study. In it, the absorption coefficient of each gray gas is given as a linear function of the partial pressure p_a of the participating mixture, $\kappa_j = \kappa_{pj} p_a$, where κ_{pj} is the pressure-based absorption coefficient of the gas, while the blackbody weighting coefficients are represented as

$$a_j(T) = \sum_{j=0}^{J} b_{j,k} T^k \,, \tag{5}$$

where $b_{i,j}$ is the polynomial coefficient of kth order for the jth gray gas. Here, the values of $b_{i,j}$ and κ_{pj} are those generated in Centeno *et al.*, 2018, for a H_2O-CO_2 mixture with constant mole fraction ratio between these species of 1.5, which is the ratio found in the stoichiometric combustion of ethanol.

3.3 Correction of the Emission Term

The radiative emission, given by the last term in Eq. (2), demands special analysis in the flame region of the fire. In LES of turbulent combustion problems, the use of large grid cells near the flame front can lead to computed temperatures considerably lower than the actual flame temperature, since its calculation is based on a bulk average for each grid cell. To account for this effect, in some of the simulations of this study a correction factor C has been introduced to the emission term, following the approach of McGrattan *et al.*, 2019a. This factor artificially increases the blackbody emission, i.e.,

$$I_b = C \frac{\sigma T(x)^4}{\pi} \,, \tag{6}$$

and is computed as

$$C = \min \left(100 \,,\, \max \left[1, \frac{\sum_{\dot{q}'''>0} (\chi_r \dot{q}''' + \kappa G) \, \mathrm{d}V}{\sum_{\dot{q}'''>0} (4\kappa\sigma T^4) \, \mathrm{d}V} \right] \right) . \tag{7}$$

In this equation, $\dot{q}'''$ is the heat release rate by combustion and χ_r is the radiant fraction of the flame (i.e., the nominal fraction of the combustion energy that is released as thermal radiation). Note that this correction is only applied in the framework of the GG model, which is why the same κ is used in the numerator and denominator of Eq. (7).

4. NUMERICAL MODELING

The set of transport equations described in the previous section are numerically solved in the open-source, Fortran-based Fire Dynamics Simulator (FDS) solver (McGrattan *et al.*, 2019b). A second-order, explicit, predictor-corrector scheme is used to advance the transient calculation in time, with the time-step size adjusted dynamically as to keep the Courant-Friedrichs-Lewy number between 0.8 and 1.0 at every grid point. Scalar convective transport is modeled employing the second-order, total variation diminishing scheme Superbee Roe (1986). More information on the numerical modeling presently adopted is reported in Fernandes *et al.*, 2020 and McGrattan *et al.*, 2019b.

The computational domain has the same dimensions as the room in the experimental configuration of Tu *et al.*, 2013, with the burner located at the center of the floor. A numerical grid with characteristic cell size of 25 mm at the flame region, and four times this size outside this region, is generated for the spatial discretization of the domain, as shown in Figure 1. A total of 400 control angles are adopted for the solution of the RTE with the FVM. These are the same discretization parameters used by Fernandes *et al.*, 2020; in that paper, it was shown that the spatial grid satisfies both the D^* and M criteria of McGrattan *et al.*, 2019a, and Pope, 2004, respectively, whereas the refinement level for the angular discretization leads to differences in the predicted radiative heat fluxes of less than 3 % relative to a finer level.

5. RESULTS

The ethanol pool fire described in Chapter 2 has been simulated for five different cases, as listed in Table 1. Four cases (GG-1 to GG-4) employ the GG model for the spectral treatment of the radiative transfer, while a fifth one (WSGG) uses the WSGG model, as described in Section 3.2. The difference between the calculations with the GG model is that GG-1 and GG-2 do not consider soot formation, but the latter includes the correction of the emission term through the radiative fraction introduced in Section 3.3, with $\chi_r = 0.2$, which is the same value used in Fernandes *et al.*, 2020. GG-3 and GG-4 differ in the same way as GG-1 and GG-2, but both consider soot formation (with a soot yield of 0.0012 g_{soot}/kg_{fuel}, again following Fernandes *et al.*, 2020). The calculation with the WSGG model also considers soot formation. A simple pyrolysis model was employed by prescribing a mass loss rate per unit area (MLRPUA) of 0.018 $kg/(m^2\,s)$ in the simulations of all cases.

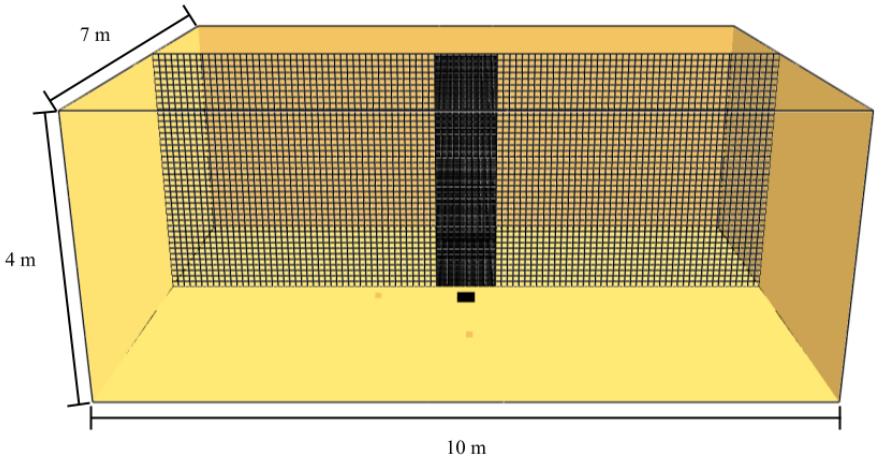

Figure 1. Computational domain and spatial grid for the simulations

Table 1. Nomenclature and differences in formulation between each case

Case	Soot formation	Emission correction
GG-1	No	No
GG-2	No	Yes
GG-3	Yes	No
GG-4	Yes	Yes
WSGG	Yes	No

According to the experimental data of Tu *et al.*, 2013, a steady burning state for this configuration is reached approximately 200 s after the start of the combustion process, and lasts for about 350 s, after which the burning rate decreases because of fuel depletion. The same was verified in the present simulations, so all data reported next are obtained by time-averaging the instantaneous results for an interval between 200 s and 600 s from the start of the numerical calculation. This long averaging period allows for several puffing cycles of the flame. Figure 2 presents the time-averaged temperatures of case GG-3 in two dimensions.

Figure 3 plots the vertical profile of the time-averaged temperature $\langle T \rangle$ along the center line of the burner (the angle brackets denote a time-averaging operation). As expected, the temperature increases until the peak, which occurs at different z positions in each tested case, and, from that point on, the temperature decreases as the height above the burner increases. This indicates that the flame height changes from case to case: the flame is shorter for the simulations with the GG model, especially when soot formation is considered and the emission correction is applied. This occurs because the radiation loss in the flame is larger for the GG model than for the WSGG model, and it is larger still when either soot formation or the emission correction are included in the calculations (this is further discussed below). A larger heat loss tends to decrease the flame temperatures—note that the peak $\langle T \rangle$ is the highest for the WSGG case, followed by GG-1—and to shrink the flame itself.

Furthermore, Fig. 3 shows that the results of the cases with the GG model are closer to each other than to those obtained with the WSGG model. This signals that, for the flame under study, the non-grayness of the participating medium is more important for the overall solution than considering soot radiation. Also, because soot radiation is basically gray (Howell *et al.*, 2016), this result indicates that soot has a smaller contribution to the overall radiative heat transfer than the gaseous phase; this has been corroborated by other studies on ethanol pool fires (Fischer and Grosshandler, 1989; Nmira *et al.*, 2020).

Comparing cases GG-2 to GG-1 and GG-4 to GG-3, it is possible to see that including the radiative emission correction led to lower temperatures. This again is expected, seeing that the C factor is always greater or equal to unity (cf. Eq. (7)), so it always acts to increase the radiative emission (and, therefore, the radiation loss) from the flame. However, also as a consequence of this, the introduction of the C factor always makes the solution distance itself from the (arguably more accurate) one obtained by the WSGG model, since, as noted above, the WSGG model always predicts smaller radiation losses than the GG model.

In Fig. 4, the time-averaged temperature and radiation loss fields (the latter given as the symmetric of $\langle S_r \rangle$) are

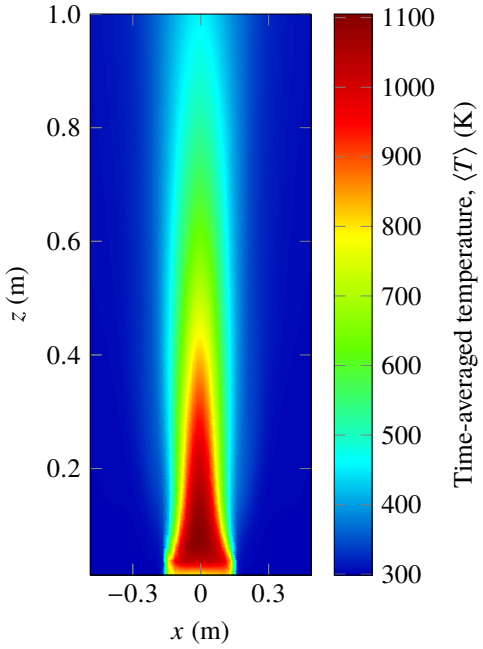

Figure 2. Time-averaged temperature for the GG-3 case

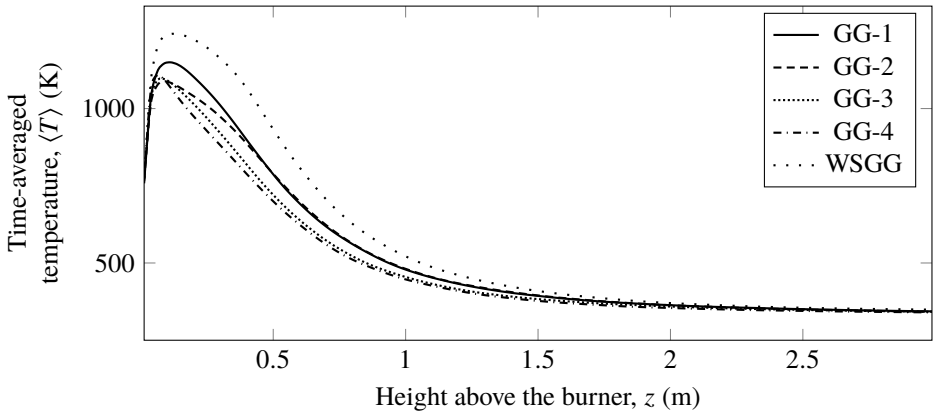

Figure 3. Time-averaged temperature along the height above the burner

shown along a horizontal line that passes through the flame axis, at different heights z above the burner. Note that these heights correspond to the vertical center of the three rows of grid cells nearest to the burner surface. Closer to the burner (z = 12.5 mm and z = 37.5 mm), two temperature peaks corresponding to the flame front are clearly visible, whereas a single peak is observed at z = 62.5 mm. It is interesting to note that, despite the fact that the radiation loss predicted by the the GG model differed significantly from that computed with the WSGG model, the temperature field obtained with the two models was much closer to each other. This can likely be explained by the fact that, for this laboratory-scale fire, other heat transfer mechanisms, particularly convection, play as an important of a role as (if not more important than) radiation.

Once again, the results for the GG model with and without soot showed a better agreement to each other than to the WSGG model, corroborating the previous observations. Note also that the radiation loss is greater for cases GG-3 and GG-4 (i.e., when soot formation is included) than for cases GG-1 and GG-2, which is to be expected since soot in known to contribute to increasing the emission of the flame (see, for instance, Cassol *et al.*, 2015). Furthermore, comparing GG-2 and GG-3 evidences that including the emission correction factor is not sufficient to increase the radiation loss to match that which is obtained by including soot formation.

In the experimental study reported by Tu *et al.*, 2013, two radiometers were used to measure the radiative heat flux from the flame. The radiometers were positioned 1.35 m to the sides of the pool in orthogonal directions and at a height 50 mm above its surface. The uncertainties associated to the measurements were $\pm 1.5\,\mathrm{W/m^2}$. Table 2 compares the experimental data and the results of each simulation, and shows that the errors associated to all calculations with the GG model fall between 12 % and 20 %. The maximum improvement caused by applying the emission correction was 2.1 % (from GG-1 to GG-2), while considering soot formation consideration reduced the error by up to 7.8 % (from GG-3 to GG-1). This once again indicates that, for the analyzed cases, the soot formation presents a more important role in the

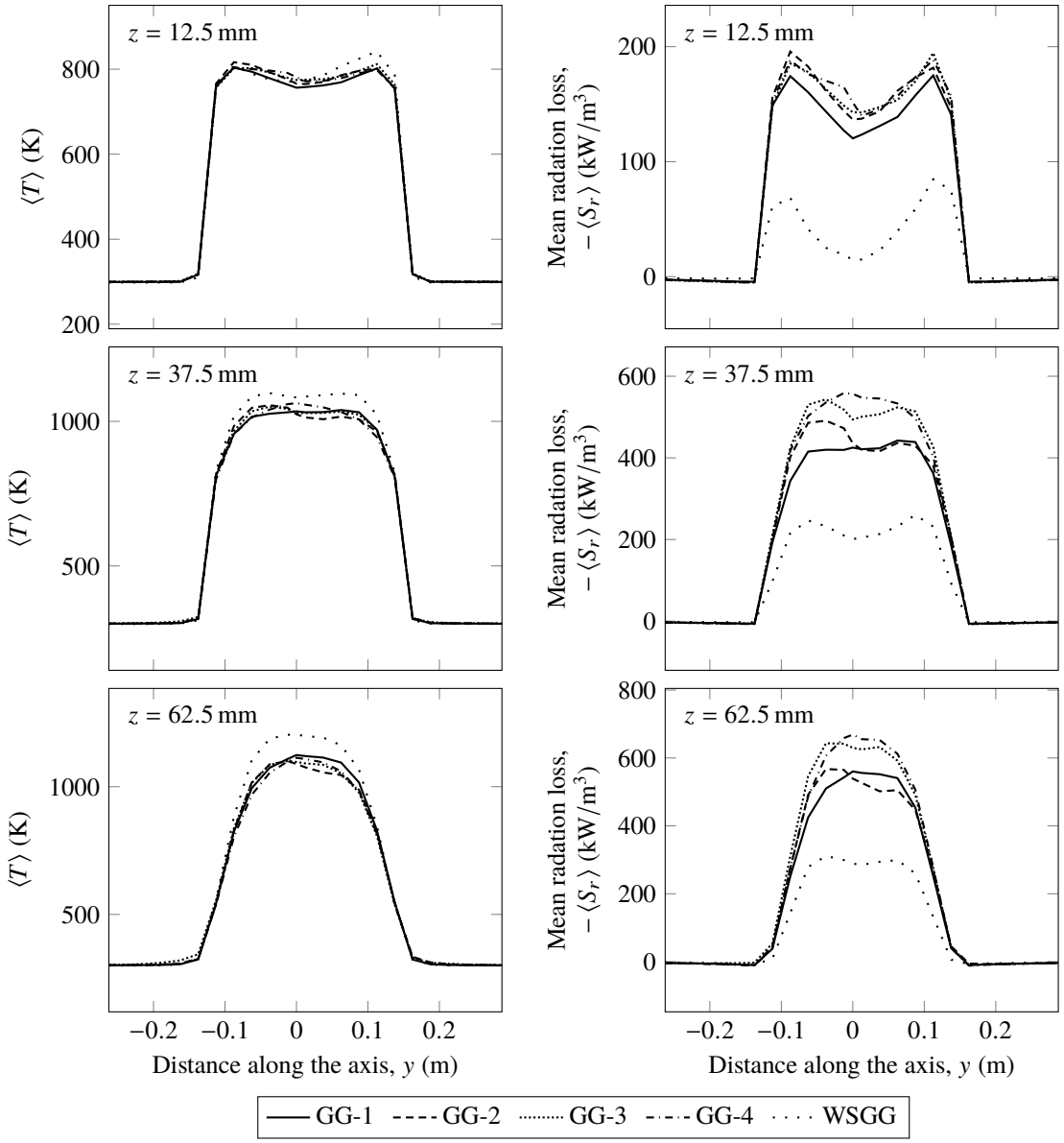

Figure 4. Time-averaged temperature and radiation heat loss along the horizontal axis at different heights above the burner

results improvement than the radiative fraction.

The simulations with the WSGG model lead to a less accurate estimate of radiation fluxes, with errors relative to the measurements of more than 50 %. However, this should not be seen as an indication that this provides a worse prediction of the radiative transfer than the GG model, which the literature has consistently shown to not be the case (Howell *et al.*, 2016; Modest, 2013). In fact, as evidenced by Fig. 4, the WSGG model predicts smaller radiation losses from the flame (and, as a consequence, smaller radiative heat fluxes at the radiometers) than the GG model, which, as noted before, is consistent with what was observed in other studies. However, because the simulations with the GG model already underestimates the radiative heat flux compared to the experimental data, this leads to an even more severe underprediction of this quantity with the WSGG model. The reason for the large differences between the simulation with the WSGG model and the experiment likely lies instead with the models used for the other physical processes involved in the simulations, some of which (such as the combustion model) involve significant simplifications. These should be further investigated in future studies.

6. CONCLUSIONS

This paper compared the gray gas and weighted-sum-of-gray-gases models for fully-coupled, large-eddy simulations of an ethanol pool fire, which were carried out in the numerical solver Fire Dynamics Simulator, based on the experimental configuration of Tu *et al.*, 2013. Four GG formulations (considering and neglecting soot radiation and a correction to the

Table 2. Comparisons between the radiometer data reported by Tu *et al.*, 2013, and the radiative heat fluxes predicted by each simulation. The deviations between simulations and the experiment (in %) are shown in parenthesis.

Case	Radiometer 1 (kW/m^2)	Radiometer 2 (kW/m^2)
Tu *et al.*, 2013	473.1 ± 1.5	473.8 ± 1.5
GG-1	382.9 (19.1)	379.8 (19.8)
GG-2	384.6 (18.7)	389.8 (17.7)
GG-3	411.3 (13.1)	417.1 (12.0)
GG-4	416.1 (12.0)	410.8 (13.3)
WSGG	218.8 (53.7)	218.9 (53.8)

radiative emission to account for coarse-grid underpredictions of the flame temperature) and a WSGG model have been implemented, with results showing that the GG simulations agree much better to each other than to the WSGG model. This gives an indication that the non-grayness of the medium is more important to the overall solution than considering soot formation, and that soot has a smaller contribution to the radiative transfer than the participating gaseous mixtures. On the other hand, for the specific simulations carried out in this paper, considering soot formation has a more significant impact over the results than including the radiative emission correction; furthermore, through comparisons with experimental data for the radiative heat flux reported in an earlier paper, it was shown that the latter improves the solution to a greater degree than the former.

The simulation with the WSGG model yielded significantly smaller radiation losses than any of the calculations with the GG model, though the differences between the temperature field itself were much smaller, likely because of the effect of other heat transfer mechanisms such as convection. Including the correction factor only contributed to increasing the differences between the solutions with the GG and WSGG models. Due to the smaller radiation losses predicted by the WSGG model, the differences to the measurements were larger for this case than they were for any of the cases with the GG models, but this is likely because of the errors introduced by the models for other physical processes used in the simulations.

7. ACKNOWLEDGMENTS

Authors FRC, FRS and GCF thank CNPq/Brazil for a research grant, a scientific initiation and doctorate scholarships, respectively.

REFERENCES

Cassol, F., Brittes, R., Centeno, F.R., da Silva, C.V. and França, F.H.R., 2015. "Evaluation of the gray gas model to compute radiative transfer in non-isothermal, non-homogeneous participating medium containing CO_2, H_2O and soot". *Journal of the Brazilian Society of Mechanical Sciences and Engineering*, Vol. 37, No. 1, pp. 163–172. doi:10.1007/s40430-014-0168-5.

Centeno, F.R., Brittes, R., Rodrigues, L.G.P., Coelho, F.R. and França, F.H.R., 2018. "Evaluation of the WSGG model against line-by-line calculation of thermal radiation in non-gray sooting medium representing an axisymmetric laminar jet flame". *International Journal of Heat and Mass Transfer*, Vol. 124. doi:10.1016/j.ijheatmasstransfer.2018.02.040.

Fernandes, C., Fraga, G., França, F. and Centeno, F., 2020. "Radiative transfer calculations in fire simulations: An assessment of different gray gas models using the software FDS". *Fire Safety Journal*, p. 103103. doi: 10.1016/j.firesaf.2020.103103.

Fischer, S.J. and Grosshandler, W.L., 1989. "Radiance, soot, and temperature interactions in turbulent alcohol fires". *Symposium (International) on Combustion*, Vol. 22, No. 1, pp. 1241–1249. doi:10.1016/s0082-0784(89)80135-3.

Germano, M., Piomelli, U., Moin, P. and Cabot, W.H., 1991. "A dynamic subgrid-scale eddy viscosity model". *Physics of Fluids A: Fluid Dynamics*, Vol. 3, No. 7, pp. 1760–1765. doi:10.1063/1.857955.

Howell, J.R., Mengüç, M.P. and Siegel, R., 2016. *Thermal Radiation Heat Transfer*. CRC press, 6th edition.

Magnussen, B.F. and Hjertager, B.H., 1977. "On mathematical modeling of turbulent combustion with special emphasis on soot formation and combustion". *Symposium (International) on Combustion*, Vol. 16, No. 1, pp. 719–729. doi: 10.1016/s0082-0784(77)80366-4.

McGrattan, K.B., Hostikka, S., Floyd, J., McDermott, R. and Vanella, M., 2019a. *Fire Dynamics Simulator – Volume 1: Mathematical Model*. National Institute of Standards and Technology, Building and Fire Research Laboratory.

McGrattan, K.B., Hostikka, S., Floyd, J., McDermott, R. and Vanella, M., 2019b. *Fire Dynamics Simulator User's Guide*. National Institute of Standards and Technology, Building and Fire Research Laboratory.

Modest, M.F., 1991. "The weighted-sum-of-gray-gases model for arbitrary solution methods in radiative transfer". *Journal*

of heat transfer, Vol. 113, No. 3, pp. 650–656. doi:10.1115/1.2910614.

Modest, M.F., 2013. *Radiative Heat Transfer*. Academic Press.

Modest, M.F. and Haworth, D.C., 2016. *Radiative Heat Transfer in Turbulent Combustion Systems: Theory and Applications*. Springer.

Nmira, F., Ma, L. and Consalvi, J.L., 2020. "Assessment of subfilter-scale turbulence-radiation interaction in non-luminous pool fires". *Proceedings of the Combustion Institute*. doi:10.1016/j.proci.2020.06.271.

Pope, S.B., 2004. "Ten questions concerning the large-eddy simulation of turbulent flows". *New Journal of Physics*, Vol. 6, No. 35, pp. 1–24. doi:10.1088/1367-2630/6/1/035.

Raithby, G.D. and Chui, E.H., 1990. "A finite-volume method for predicting a radiant heat transfer in enclosures with participating media". *Journal of Heat Transfer*, Vol. 112, pp. 415–423. doi:10.1115/1.2910394.

Roe, P.L., 1986. "Characteristic-based schemes for the euler equations". *Annual Review of Fluid Mechanics*, Vol. 18, pp. 337–365. doi:10.1146/annurev.fl.18.010186.002005.

Tu, R., Fang, J., Zhang, Y.M., Zhang, J. and Zeng, Y., 2013. "Effects of low air pressure on radiation-controlled rectangular ethanol and n-heptane pool fires". *Proceedings of the Combustion Institute*, Vol. 34, No. 2, pp. 2591–2598.